frontiers in Forests and Global Change

TYPE Original Research
PUBLISHED 16 July 2026
DOI 10.3389/ffgc.2026.1879552

Check for updates

OPEN ACCESS

EDITED BY
Aldo Rafael Martínez Sifuentes,
National Institute of Forestry and Agricultural Research (INIFAP), Mexico

REVIEWED BY
Fatima Zohra Tebbi,
University of Batna 2, Algeria
Ahmet Faruk İpek,
Istanbul Technical University, Türkiye

*CORRESPONDENCE
Abdalrahman Ahmed
ix3mzk@uni-sopron.hu;
omda33sd@gmail.com

RECEIVED 12 May 2026
REVISED 23 June 2026
ACCEPTED 29 June 2026
PUBLISHED 16 July 2026

CITATION
Ahmed A and Czimber K (2026) Multi-scale drought-vegetation relationships in the Jebel Marra Highlands, Sudan: evidence from Landsat NDVI time series, SPEI, and BFAST analysis.
Front. For. Glob. Change 9:1879552.
doi: 10.3389/ffgc.2026.1879552

COPYRIGHT
© 2026 Ahmed and Czimber. This is an open-access article distributed under the terms of the Creative Commons Attribution License (CC BY). The use, distribution or reproduction in other forums is permitted, provided the original author(s) and the copyright owner(s) are credited and that the original publication in this journal is cited, in accordance with accepted academic practice. No use, distribution or reproduction is permitted which does not comply with these terms.

Multi-scale drought-vegetation relationships in the Jebel Marra Highlands, Sudan: evidence from Landsat NDVI time series, SPEI, and BFAST analysis

Abdalrahman Ahmed[1,2]* and Kornel Czimber[1]

[1]Faculty of Forestry, Institute of Geomatics and Civil Engineering, University of Sopron, Sopron, Hungary, [2]Department of Forest and Environment, Faculty of Forest Sciences and Technology, University of Gezira, Wad Madani, Sudan

Dryland ecosystems are highly sensitive to climatic variability, particularly drought, which influences vegetation productivity, ecosystem function, and land degradation processes. Understanding vegetation–drought relationships is therefore important for assessing ecosystem dynamics in semi-arid environments. This study investigated long-term vegetation dynamics and drought conditions in the Jebel Marra Highlands of western Sudan using Landsat-derived Normalized Difference Vegetation Index (NDVI) time series and multi-scale Standardized Precipitation–Evapotranspiration Index (SPEI) data for the period 2000–2024. Monthly NDVI time series were derived from Landsat imagery, while SPEI was calculated from Climate Hazards Group InfraRed Precipitation with Station Data (CHIRPS) precipitation and ERA5-Land potential evapotranspiration datasets for 3-, 6-, and 12-month accumulation periods. Temporal trends were evaluated using the Mann–Kendall test, vegetation–drought relationships were examined using correlation and lagged-correlation analyses, and vegetation regime shifts were identified using the Breaks For Additive Seasonal and Trend (BFAST) method. The NDVI time series exhibited a significant positive long-term trend ($\tau = 0.24$, $p < 0.001$), indicating an overall increase in vegetation greenness during the study period despite substantial interannual variability. Contemporaneous correlation analysis identified a significant positive relationship between NDVI and SPEI-3 ($r = 0.442$, $p < 0.001$), whereas relationships with SPEI-6 ($r = -0.074$, $p = 0.191$) and SPEI-12 ($r = 0.044$, $p = 0.443$) were not significant. Lagged-correlation analysis showed varying temporal associations among drought timescales, with maximum correlations occurring at a lag of 2 months for SPEI-3 ($r = 0.833$) and 3 months for SPEI-6 ($r = 0.868$). BFAST analysis identified consistent vegetation breakpoints around 2006–2007, 2012, and 2018 across multiple model parameterizations in the tropics. Seasonal analyses showed lower NDVI values during drought periods, particularly during the peak growing season (July–September). Overall, the results demonstrate that vegetation variability in the Jebel Marra Highlands was more strongly associated with short-term moisture conditions than with concurrent medium- or long-term droughts. The identified structural changes in the NDVI time series indicate periods of substantial vegetation reorganization during the study period. The integration of Landsat observations, locally derived SPEI datasets, and breakpoint analysis provides a useful framework for monitoring vegetation dynamics and hydroclimatic variability in semi-arid mountain environments.

KEYWORDS
BFAST, climate variability, drought, dryland ecosystems, ecosystem resilience, Sudan, vegetation dynamics

1 Introduction

Dryland ecosystems are among the most climate-sensitive environments globally, where vegetation productivity and ecosystem function are strongly constrained by water availability and hydroclimatic variability (Dai, 2011; Dutra et al., 2025; Stringer et al., 2021; Wang et al., 2026). In semi-arid regions, prolonged drought events can substantially alter vegetation structure, reduce ecosystem productivity, and trigger long-term ecological degradation (IPCC, 2023). These impacts are particularly pronounced across the African Sahel, where increasing climatic variability, recurrent droughts, and rising temperatures have intensified ecological vulnerability in recent decades (Herrmann et al., 2005; Nicholson et al., 2013).

The Sahel has historically experienced severe drought episodes, especially during the 1970s and the 1980s, causing extensive vegetation decline, land degradation, and socio-economic disruption (Anyamba and Tucker, 2005). However, satellite observations since the late twentieth century have also revealed localized vegetation recovery and "Sahel greening" trends linked to partial rainfall recovery, land-use changes, and ecosystem adaptation processes (Brandt et al., 2015; Dardel et al., 2014). Despite these regional greening signals, vegetation responses remain highly heterogeneous due to differences in topography, land management, climatic gradients, and anthropogenic disturbances (Fensholt et al., 2012).

Therefore, understanding vegetation–drought interactions is essential for assessing ecosystem resilience, climate adaptation, and land degradation risk in dryland regions. Satellite remote sensing has become one of the most effective approaches for monitoring vegetation dynamics over large spatial and temporal scales. In particular, the Normalized Difference Vegetation Index (NDVI) has been widely used to assess vegetation greenness, productivity, and ecosystem responses to environmental change because of its long-term availability and compatibility with multiple satellite missions (Mehmood et al., 2024; Pettorelli et al., 2005; Zeng et al., 2022). When combined with drought indicators such as the Standardized Precipitation Evapotranspiration Index (SPEI), remote sensing observations provide valuable insights into the effects of moisture deficits on ecosystem functioning across multiple temporal scales (Vicente-Serrano et al., 2010).

Recent studies have demonstrated that vegetation responses to drought are often scale-dependent and may exhibit delayed effects owing to soil moisture storage, groundwater dynamics, and physiological memory (Hua et al., 2019; Jiang et al., 2023; Liu, 2024). Moreover, repeated drought exposure can trigger abrupt ecological transitions and vegetation regime shifts when resilience thresholds are exceeded, particularly in semi-arid environments characterized by recurrent hydroclimatic stress (El Kenawy, 2024; Ma et al., 2020; Shi et al., 2026). The detection of nonlinear ecosystem responses is increasingly important for understanding ecological stability under ongoing climate change.

Recent drought research has also emphasized the value of integrating multiple indicators, including meteorological drought indices, vegetation metrics, land-use information, and disturbance records, to improve the understanding of ecosystem vulnerability and drought risk (Agustiyara et al., 2026; Blauhut et al., 2016; Fathi-Taperasht et al., 2023). Although such integrated approaches provide a comprehensive assessment of environmental change, studies focusing on vegetation–drought relationships remain an essential step toward identifying the climatic mechanisms underlying ecosystem responses, particularly in data-limited dryland regions such as the Mediterranean.

In Sudan, drought remains one of the most significant environmental hazards affecting ecosystem productivity, food security and land sustainability (Alriah et al., 2024). Western Sudan, particularly the Darfur region, is highly vulnerable because of its semi-arid climate, high rainfall variability, and dependence on rain-fed livelihoods. Previous studies in Sudan have identified strong linkages between climatic variability and vegetation dynamics using remote sensing approaches, with NDVI trends closely associated with rainfall fluctuations and drought conditions (Ahmed et al., 2025; Ahmed et al., 2025). Nevertheless, relatively limited attention has been given to montane dryland ecosystems such as Jebel Marra, where complex topographies and localized microclimates may generate distinct ecological responses to drought.

Jebel Marra represents one of the most ecologically important highland systems in the Sahelian Zone. Owing to its elevated terrain and localized rainfall enhancement, the region supports relatively dense vegetation and functions as an ecological refuge within the surrounding semi-arid landscape (Hegazy et al., 2018b). Simultaneously, the region has experienced prolonged armed conflict, population displacement, agricultural abandonment, and changing land-use practices since the early 2000s (Abdul-Jalil and Unruh, 2013; UNEP, 2024). These factors may interact with climatic variability to influence the dynamics of vegetation. However, while conflict-related processes provide important contextual information, quantifying their contribution is beyond the scope of the present study, which specifically focuses on drought–vegetation relationships.

Although several studies have investigated vegetation dynamics in conflict-affected regions of Darfur (Ahmed et al., 2026; Ahmed et al., 2024), few have explicitly examined the temporal relationships between drought variability and vegetation responses using long-term Landsat observations. In particular, the relative importance of drought timescales, delayed vegetation responses, and abrupt vegetation regime shifts remain poorly understood in the Jebel Marra ecosystem.

To address these knowledge gaps, this study integrated multi-decadal Landsat-derived NDVI observations with multi-scale SPEI drought indices derived from CHIRPS precipitation and ERA5-Land potential evapotranspiration to investigate vegetation dynamics in the Jebel Marra region during 2000–2024. Specifically, the objectives were as follows: (1) quantify long-term vegetation dynamics and drought variability, (2) examine relationships between vegetation greenness and drought across multiple temporal scales, (3) evaluate lagged vegetation responses to drought conditions, (4) identify abrupt vegetation regime shifts using breakpoint analysis, and (5) assess vegetation responses under different drought severity classes. By integrating long-term remote sensing observations with multi-scale drought metrics, this study contributes to an improved understanding of ecosystem resilience, drought sensitivity, and ecological change in conflict-affected dryland mountain environments in the African Sahel.

2 Methodology

2.1 Study area

This study was conducted in the Jebel Marra region of Central Darfur in Western Sudan. The study area is geographically located between 12°48′–13°24′N and 24°00′–24°48′E (Figures 1a,b). The study area covered approximately 3280.279 km^2. Jebel Marra forms part of the Sahelian ecotone, a transitional climatic and ecological zone situated between the hyper-arid Sahara Desert to the north and the more humid savanna woodlands to the south (Ahmed, 1983; Williams, 2021).

Jebel Marra is characterized by a semi-arid climate with high seasonal rainfall variability. The mean annual precipitation ranges between approximately 520 and 672 mm, with rainfall concentrated primarily during the June–September wet season, whereas the mean daily temperatures range from 23 to 26 °C (FAO, 2015). Therefore, vegetation growth in this region is strongly controlled by seasonal water availability and interannual rainfall fluctuations.

Topographically, the region consists of a volcanic highland complex rising above 3,000 m above sea level, forming one of the most elevated landscapes in Sudan (Hegazy et al., 2018a). The pronounced elevation gradient generates localized microclimatic conditions that support vegetation that is denser than that of the surrounding lowland plains. The landscape comprises rugged mountains, sandy-clay plains, valleys, and ephemeral stream systems (wadis), including Wadi El Ku, Wadi Ibra, and Wadi Azum, which contribute to the Lake Chad Basin hydrological network (Hamid Ali, 2014; Knight, 2023).

Ecologically, the region supports heterogeneous savanna vegetation dominated by woody species, such as *Acacia senegal*, *Albizia amara*, Anogeissus leiocarpus, *Balanites aegyptiaca*, and *Eucalyptus* spp. Several of these species exhibit strong vegetative regeneration capacity through basal resprouting, which enhances ecosystem resilience following disturbances such as drought, fire, grazing, and wood harvesting (Ahmed et al., 2025).

In addition to climatic stressors, the region has experienced prolonged armed conflict since the early 2000s, resulting in major socio-ecological transformations. Conflict-driven displacement, agricultural abandonment, and altered land-use practices have modified vegetation dynamics across the landscape (Abdul-Jalil and Unruh, 2013; UNEP, 2024). Reduced agricultural pressure in some areas may have facilitated natural vegetation recovery, whereas concentrated resource exploitation near internally displaced persons (IDP) camps has accelerated localized degradation (van Deetjen, 2020; Kamta et al., 2020).

The combined influence of climatic variability, ecological heterogeneity, and conflict-related land-use change makes Jebel Marra a particularly important natural laboratory for investigating drought–vegetation interactions in dryland mountain ecosystems.

2.2 Landsat NDVI data and time-series construction

Vegetation dynamics were characterized using a continuous monthly NDVI time series derived from Landsat imagery spanning from January 2000 to December 2024. The analysis integrated atmospherically corrected surface reflectance products from Landsat 5 Thematic Mapper (TM), Landsat 7 Enhanced Thematic Mapper Plus (ETM+), and Landsat 8 Operational Land Imager (OLI) available through the United States Geological Survey (USGS) Landsat Collection 2 archive and accessed via the Google Earth Engine (Gorelick et al., 2017). Landsat imagery was selected because of its long-term temporal continuity, global availability, and moderate spatial resolution (30 m), making it well suited for monitoring vegetation

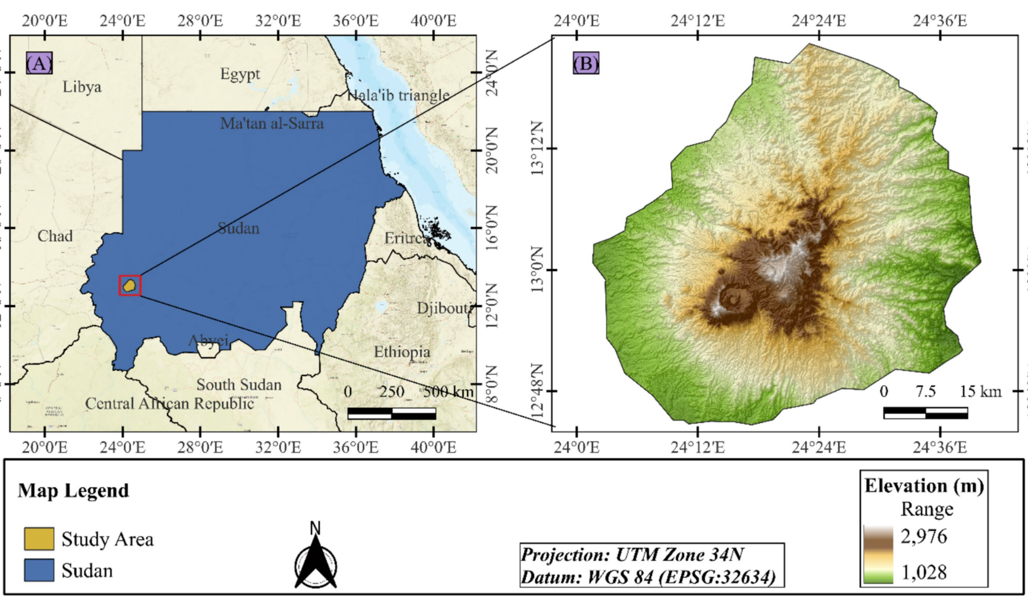

FIGURE 1
Map of the study area showing **(A)** location of the Jebel Marra Highlands in western Sudan, and **(B)** the elevation amp of the study area. Coordinates are displayed in the Geographic Coordinate System WGS 84 (EPSG: 32635).

dynamics in heterogeneous dryland environments (Wulder et al., 2019; Ye et al., 2025). Atmospherically corrected Landsat Collection 2 Surface Reflectance products were used throughout the analysis to maximize the consistency among sensors and minimize inter-sensor radiometric differences. Previous studies have shown that although Landsat TM, ETM+, and OLI sensors exhibit high radiometric agreement, small systematic differences may remain among the sensors and should be considered when interpreting long-term vegetation trends (Roy et al., 2016). Cloud-contaminated observations were removed using the quality assessment (QA) bands provided in the Landsat Collection 2 archive. The NDVI was calculated using Equation 1.

$$NDVI = \frac{NIR - Red}{NIR + Red} \tag{1}$$

Where: *NIR* is the Near-Infrared reflectance, and *Red* is the reflectance of the red band, respectively (Rouse et al., 1974).

Monthly NDVI composites were generated by aggregating all cloud-free observations for each month. Spatial averages were subsequently extracted from the study area to produce a continuous regional vegetation time-series. Missing observations were interpolated using linear interpolation followed by spline fitting to maintain temporal continuity. To assess the magnitude of temporal gaps, the frequency of missing monthly observations was quantified before interpolation. Of the 312 monthly observations available from 2000 to 2024, 17 months (5.45%) contained missing value. Missing observations were concentrated in a limited number of years, with the highest occurrence in 2003 (5 months) and 2009 (3 months), whereas most years contained zero or one missing month (Supplementary Table S1). Following interpolation and smoothing, a complete monthly NDVI time series was obtained for the subsequent analyses.

Although Landsat Collection 2 Surface Reflectance products provide substantial radiometric consistency among sensors, explicit cross-sensor harmonization coefficients were not applied. Therefore, a transition analysis was conducted to evaluate whether the Landsat 7–8 sensor transition introduced an artificial discontinuity in the NDVI time series. To evaluate potential discontinuities associated with the Landsat 7–8 transition, a linear regression model including both the temporal trend and a sensor-transition indicator variable was fitted to the NDVI time series. The significance of the transition coefficient was used to assess whether the sensor change introduced an abrupt shift in NDVI values. The significance of the transition coefficient was evaluated to determine whether the Landsat 7–8 transition introduced an abrupt sensor-related discontinuity in vegetation records.

To reduce residual atmospheric noise while preserving seasonal and interannual variability, the NDVI time series was smoothed using a Savitzky–Golay (SG) filter with a third-order polynomial and a nine-month moving window. The SG filter has been widely applied in vegetation time-series analysis because it effectively suppresses noise while preserving phenological characteristics and local extrema (Chen et al., 2004; Liu et al., 2022). The monthly NDVI anomalies were calculated using Equation 2.

$$\mathrm{NDVI}_{anom,i} = \mathrm{NDVI}_i - \mathrm{NDVI}_{month} \tag{2}$$

Where NDVI_i is the monthly NDVI value, and NDVI_{month} is the long-term mean NDVI for the corresponding calendar month. This anomaly approach isolates vegetation deviations associated with drought stress and ecological disturbances.

2.3 Drought assessment using SPEI derived from CHIRPS and ERA5-land data

Drought conditions were quantified using the SPEI, a multiscale drought indicator that incorporates both precipitation and atmospheric evaporative demand and is widely used to assess drought impacts under varying climatic conditions (Vicente-Serrano et al., 2010).

Monthly precipitation data were obtained from the CHIRPS dataset, and potential evapotranspiration (PET) data were derived from the ERA5-Land Monthly Aggregated reanalysis product. Both datasets were accessed and processed using the Google Earth Engine (GEE) cloud-computing platform (Gorelick et al., 2017).

CHIRPS provides quasi-global precipitation estimates at a spatial resolution of approximately 0.05° (~5 km) by integrating satellite observations within situ station measurements, making it particularly suitable for hydroclimatic analyses in data-scarce regions (Funk et al., 2015). ERA5-Land provides monthly land surface hydrometeorological variables, including potential evapotranspiration, at a spatial resolution of approximately 0.1° (~9 km) and has been widely applied in drought and ecosystem studies (Muñoz-Sabater et al., 2021). Although ERA5-Land provides spatially consistent estimates of potential evapotranspiration, previous studies have reported a tendency to overestimate atmospheric evaporative demand in some arid and semi-arid environments; therefore, uncertainty associated with PET estimates should be considered when interpreting drought conditions (Muñoz-Sabater et al., 2021).

The analysis was conducted for the period January 2000 to December 2024, corresponding to the common temporal availability of both datasets. The monthly precipitation totals were calculated by aggregating the daily CHIRPS observations within each calendar month. Monthly PET values were extracted from ERA5-Land and converted from meters to millimeters by multiplying them by 1,000. Because ERA5-Land stores evapotranspiration fluxes as negative values, the PET values were multiplied by −1 to obtain positive values.

Monthly climatic water balance (D) was calculated using Equation 3:

$$D = P - PET \tag{3}$$

Where *P* represents monthly precipitation (mm) and *PET* represents monthly potential evapotranspiration (mm).

The accumulated climatic water-balance series was transformed into SPEI values using the SPEI package in R following the methodology of Vicente-Serrano et al. (2010). A log-logistic probability distribution was fitted to the accumulated water-balance series and subsequently transformed into standardized normal variates to derive SPEI-3, SPEI-6, and SPEI-12. These accumulation periods were selected to represent different drought processes and ecological response times.

- SPEI-3: Short-term meteorological drought.
- SPEI-6: Medium-term agricultural drought.
- SPEI-12: Long-term hydrological and ecological drought.

The use of multiple SPEI timescales enables the assessment of both immediate and delayed vegetation responses to moisture deficits and provides a framework for evaluating drought impacts across different temporal dimensions of ecosystem functions.

2.4 Classification of drought severity

Drought severity classes were defined according to the standard SPEI thresholds commonly used in climatological and ecological drought studies (Vicente-Serrano et al., 2010) including mild drought ($-1.0 < \text{SPEI} \leq -0.5$), moderate drought ($-1.5 < \text{SPEI} \leq -1.0$), severe drought ($-2.0 < \text{SPEI} \leq -1.5$), and extreme drought ($\text{SPEI} \leq -2.0$). Each month within the study period was assigned a drought severity category based on the SPEI-12 values. Months with $\text{SPEI} > -0.5$ were classified as non-drought conditions and excluded from the drought severity comparisons.

2.5 Detection of vegetation regime shifts

Abrupt changes in vegetation dynamics were identified using the Breaks For Additive Seasonal and Trend (BFAST) approach (Verbesselt et al., 2010). BFAST decomposes a time series into trend, seasonal, and remainder components while simultaneously identifying statistically significant structural breakpoints.

The smoothed NDVI time series was analyzed using a harmonic seasonal model. A minimum segment size corresponding to 15% of the total time-series length ($h = 0.15$) was used in the primary analysis. To evaluate the robustness of the identified breakpoints, a sensitivity analysis was conducted using h values of 0.10 and 0.20. Breakpoints that remained consistent across the parameterizations were considered robust indicators of structural change in vegetation dynamics.

The detected breakpoints were interpreted as indicators of structural changes in vegetation dynamics. BFAST has been widely used to identify abrupt changes and temporal discontinuities in ecological time-series data (Ma et al., 2020; Yao et al., 2025).

2.6 Vegetation responses to drought severity

Vegetation responses to drought were quantified using NDVI anomalies during the drought periods. For each drought severity class, the mean NDVI anomaly, standard deviation, and sample size were calculated to characterize the magnitude and variability of vegetation responses. Because NDVI anomaly distributions may deviate from normality, non-parametric statistical methods were used. Differences among the drought severity classes were evaluated using the Kruskal–Wallis rank-sum test. Where significant differences were detected, pairwise Wilcoxon rank-sum tests with Benjamini–Hochberg correction were applied to control for the false discovery rate.

2.7 Lagged relationships between vegetation and drought

To investigate the delayed vegetation responses to drought. Lagged Pearson correlation analyses were conducted between the standardized smoothed NDVI time series and SPEI at 3-, 6-, and 12-month timescales. Correlations were calculated for lags ranging from 0 to 6 months to evaluate temporal associations between vegetation variability and drought conditions. To evaluate the influence of temporal autocorrelation on correlation significance, effective degrees of freedom were estimated following standard time-series correction procedures, and significance levels were reassessed using an adjusted sample size. Additionally, the Benjamini–Hochberg false discovery rate (FDR) correction was applied to account for multiple tests across lagged correlations.

A rolling correlation analysis using a 24-month moving window was also performed for SPEI-3, SPEI-6, and SPEI-12 to evaluate the temporal changes in vegetation–drought coupling during major drought episodes and the ecological transitions. These approaches are commonly used to examine temporal variability in vegetation–climate relationships and potential lagged associations in dryland ecosystems (Bunting et al., 2017; Kusch et al., 2022).

All statistical analyses, time-series processing, and visualizations were conducted using R statistical environment (R Core Team, 2020). Time-series decomposition and breakpoint detection were implemented using the bfast package, whereas smoothing, interpolation, and correlation analyses were performed using the signal, zoo, tidyverse, and related packages. Figures were standardized to the 2000–2024 study period to ensure temporal consistency across the datasets. Integrated visualizations combining NDVI anomalies, drought severity classes, SPEI dynamics, lagged correlations, and BFAST breakpoints were developed to support the analysis of vegetation variability and drought conditions throughout the study period.

3 Results

3.1 Temporal dynamics of vegetation greenness and drought variability

The monthly NDVI time series exhibited pronounced seasonal variability and a gradual increase in vegetation greenness during the 2000–2024 study period (Figure 2a). Higher NDVI values occurred during and immediately after the rainy season, whereas lower values were recorded during the dry season.

The Mann–Kendall trend test identified a significant positive monotonic trend in the NDVI ($\tau = 0.24$, $p < 0.001$). Interannual variability was observed throughout the study period, with alternating periods of positive and negative departures from the long-term mean.

NDVI anomaly analysis identified several periods of below-average vegetation activity that occurred during intervals of negative SPEI values (Figure 2b).

3.2 NDVI–drought relationships across time scales

Correlation analysis revealed contrasting relationships between NDVI and SPEI across drought timescales (Table 1). A statistically significant positive correlation was observed between NDVI and SPEI-3 ($r = 0.442$, $p < 0.001$). The correlations between NDVI and SPEI-6 ($r = -0.074$, $p = 0.191$) and NDVI and SPEI-12 ($r = 0.044$, $p = 0.443$) were not statistically significant.

Following the effective degrees-of-freedom correction, the correlation between NDVI and SPEI-12 remained non-significant ($p = 0.813$).

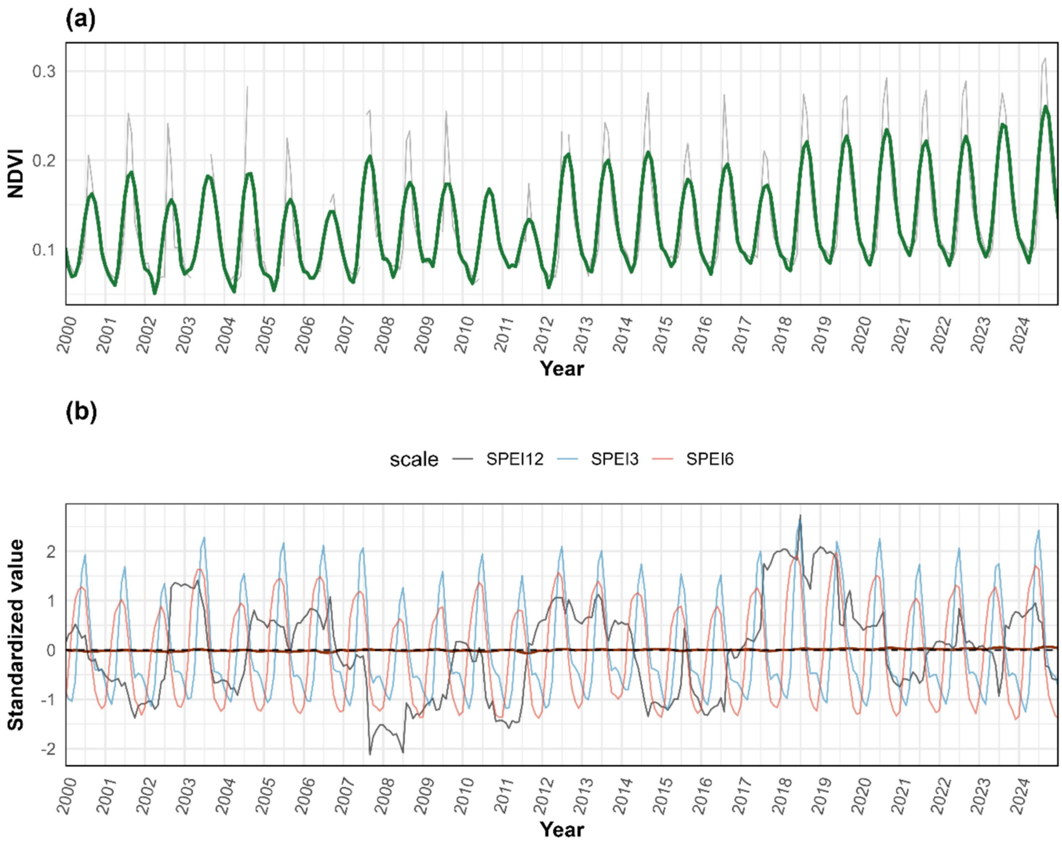

FIGURE 2
Multi-scale vegetation dynamics and drought responses in the Jebel Marra region (2000–2024). **(a)** Monthly Landsat-derived NDVI time series showing raw observations and Savitzky–Golay smoothed trends, and **(b)** NDVI anomalies relative to the long-term monthly climatology compared with SPEI-3, SPEI-6, and SPEI-12 drought indices.

TABLE 1 Correlation between NDVI and SPEI at multiple time scales.

Drought index	Correlation (r)	*p*-value
SPEI-3	0.442	0.001
SPEI-6	−0.074	0.191
SPEI-12	0.044	0.443

TABLE 2 Laged NDVI-SPEI correlation (r) by drought time scale.

Scale	0	1	2	3	4	5	6
SPEI-3	0.442	0.733	0.833	0.668	0.297	−0.136	−0.470
SPEI-6	−0.074	0.336	0.683	0.868	0.820	0.551	0.156
SPEI-12	0.044	0.065	0.089	0.109	0.124	0.129	0.141

The lagged correlation coefficients varied among the drought timescales (Table 2; Figure 3a). For SPEI-3, the correlation coefficients increased from $r = 0.442$ at lag 0 to $r = 0.833$ at lag 2 months and then declined. For SPEI-6, the coefficients increased from $r = -0.074$ at lag 0 to $r = 0.868$ at lag 3 months. For SPEI-12, the coefficients ranged from $r = 0.044$ at lag 0 to $r = 0.141$ at lag 6 months.

Following the Benjamini–Hochberg correction, significant correlations were retained for SPEI-3 (lags 0–6), SPEI-6 (lags 1–6), and SPEI-12 (lags 4–6). Rolling-correlation values varied through time for all three SPEI timescales (Figure 3b).

To account for temporal autocorrelation, lagged correlations were re-evaluated using effective degrees-of-freedom corrections. For SPEI-3, significant correlations remained at lags 0–4 after correction ($p < 0.05$). For SPEI-6, significant correlations remained at lags 1–5, including the maximum correlation observed at lag 3 ($r = 0.868$, $p < 0.001$). In contrast, the correlations between NDVI and SPEI-12 remained non-significant across all lags after autocorrelation correction (adjusted $p > 0.45$).

3.3 Detection of vegetation regime shifts

BFAST analysis identified three breakpoints in the NDVI trend component occurring around 2006–2007, 2012, and 2018 (Figure 4a).

Sensitivity analysis using alternative BFAST parameter values ($h = 0.10$, 0.15, and 0.20) identified the same three breakpoints for all model configurations. An additional breakpoint near 2003 was detected only when $h = 0.10$.

The breakpoints occurred during periods characterized by negative SPEI values and negative NDVI anomalies.

3.4 Seasonal vegetation responses under drought conditions

Monthly NDVI distributions differed between the drought and non-drought periods (Figure 4b). NDVI values during drought periods were generally lower for most months of the year. The largest differences between drought and non-drought conditions occurred in

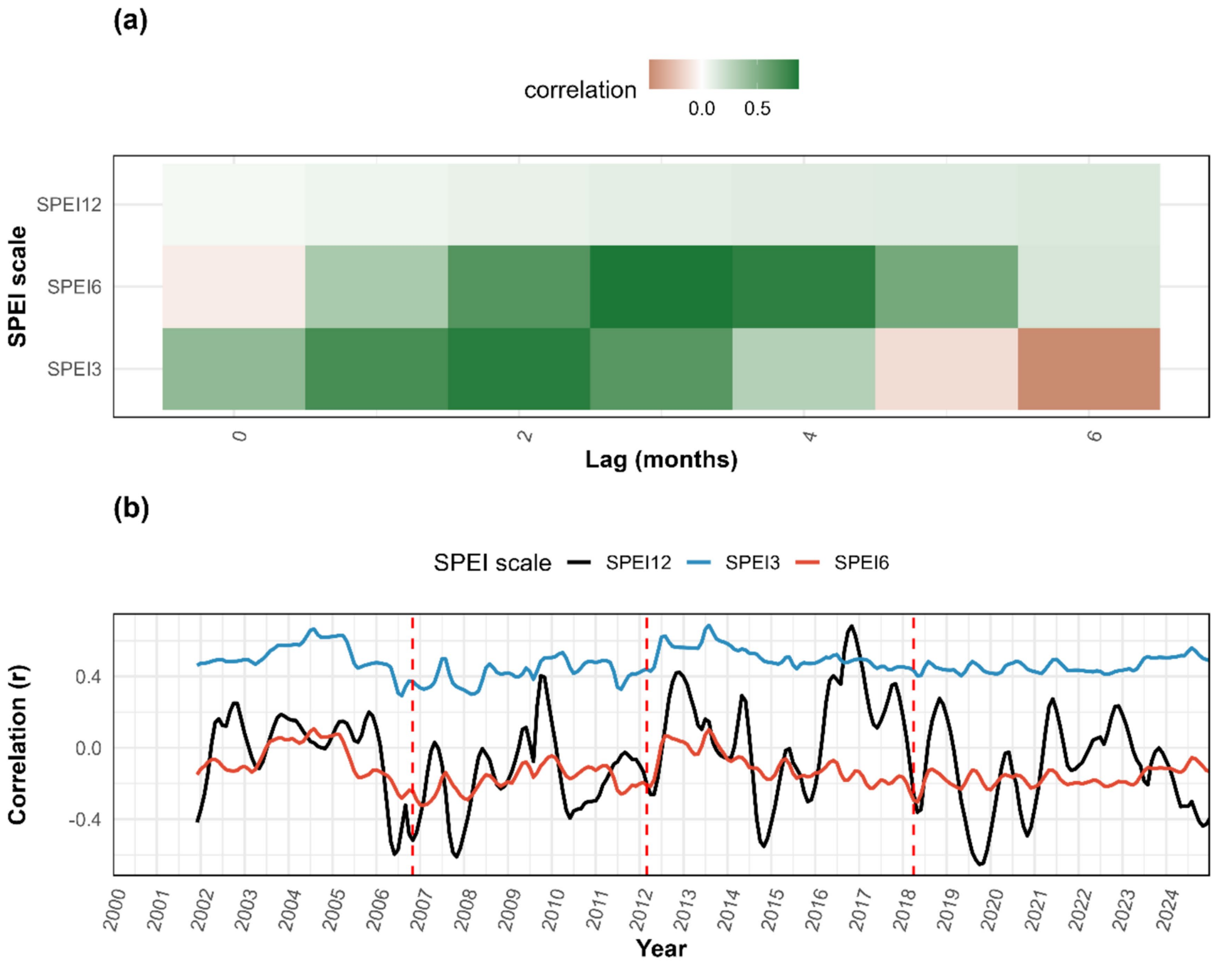

FIGURE 3
Multi-scale vegetation dynamics and drought responses in the Jebel Marra region (2000–2024). **(a)** Lagged correlation responses between standardized NDVI and multi-scale SPEI indices, and **(b)** rolling 24-month correlation between NDVI and SPEI-6 showing temporal variability in vegetation–drought coupling.

July, August, and September. The spread of NDVI values was greater during drought periods for several months.

3.5 Characteristics of drought events and associated vegetation responses

Seven drought events were identified from the SPEI-12 time series data from 2000 to 2024 (Table 3). The event duration ranged from 1 to 19 months. Mean drought intensity ranged from −1.14 to −1.52, whereas the cumulative drought severity ranged from −1.25 to −28.80. Mean NDVI anomaly values during drought events ranged from −0.016 to 0.012.

3.6 Vegetation response to drought severity

The mean NDVI anomalies varied among the drought severity classes (Table 4). The mean anomalies were −0.005 for extreme droughts, −0.004 for severe droughts, −0.005 for moderate droughts, and 0.002 for mild droughts, respectively.

The Kruskal–Wallis test indicated no statistically significant differences in NDVI anomalies among the drought severity classes ($\chi^2 = 0.40$, df = 3, $p = 0.94$). When presented together with drought classifications and breakpoint locations (Figure 5), periods of positive and negative NDVI anomalies occurred across all drought categories.

3.7 Assessment of Landsat sensor transition

Comparisons of NDVI observations during the Landsat transition period (2012–2014) revealed significant differences between Landsat 7 and Landsat 8 observations (Wilcoxon rank-sum test, $p = 0.030$). Cliff's delta indicated a moderate effect size ($\delta = -0.43$; 95% CI: −0.71 to −0.03). Comparisons of smoothed NDVI values during 2011–2015 also identified significant differences between the sensor periods (Welch's t-test, $p = 0.022$; Wilcoxon rank-sum test, $p = 0.018$). A regression model including both temporal trend and a sensor-transition indicator produced a non-significant transition coefficient ($\beta = 0.0076$, $p = 0.462$), whereas the temporal trend term remained significant ($p = 0.0066$).

4 Discussion

This study examined vegetation–drought interactions in the Jebel Marra highlands using multi-decadal Landsat NDVI observations and locally derived multi-scale SPEI indices based on CHIRPS

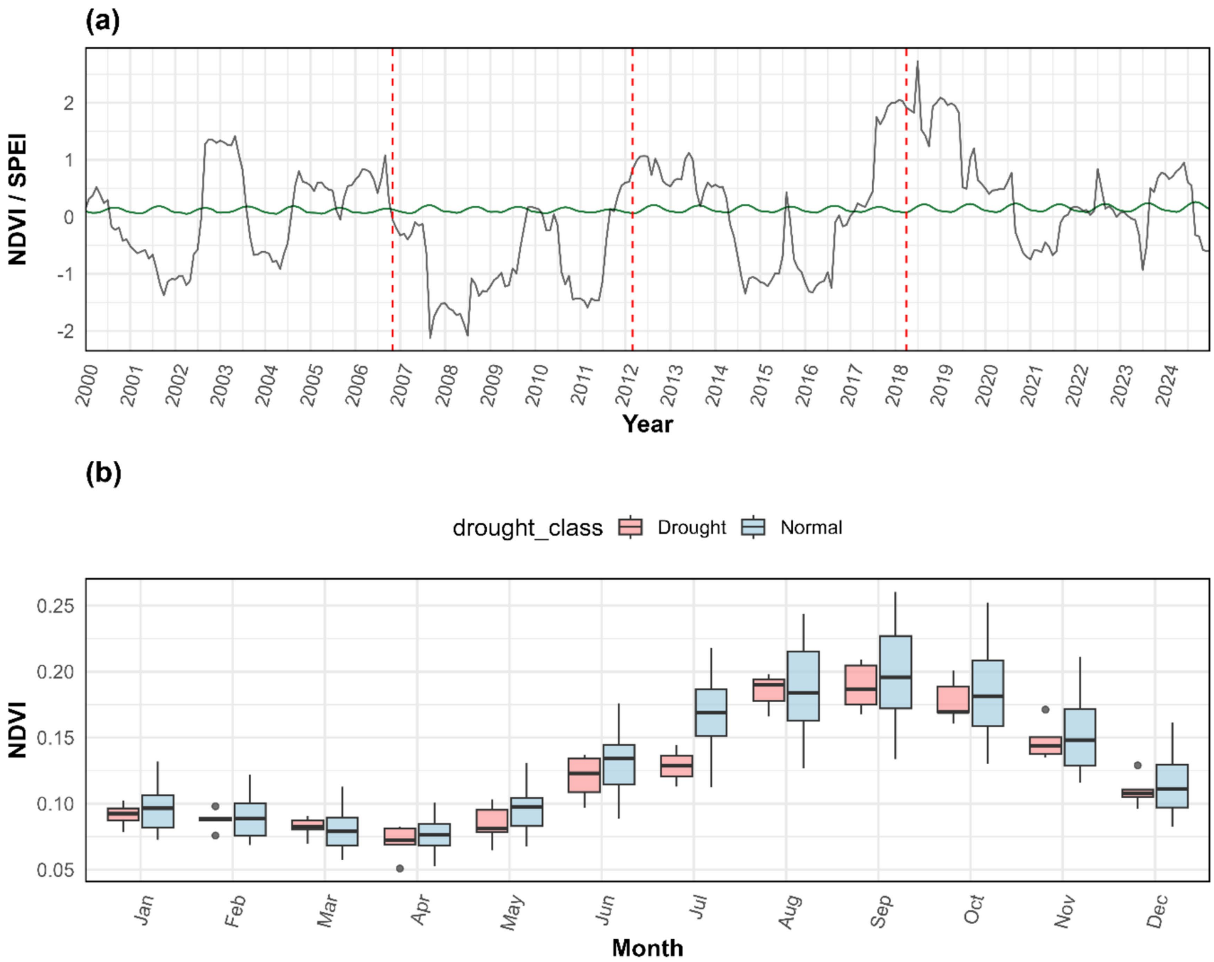

FIGURE 4
Vegetation regime shifts and seasonal drought effects in the Jebel Marra region. **(a)** BFAST-detected structural breakpoints in NDVI trends overlaid with SPEI-12. **(b)** Seasonal distribution of NDVI under drought (SPEI-12 ≤ −1) and non-drought conditions.

TABLE 3 Characteristics of identified drought events based on SPEI-12.

Event	Duration (months)	Intensity	Severity	Mean NDVI loss
1	9	−1.143222	−10.289	−0.016
2	19	−1.515684	−28.798	−0.006
3	2	−1.209500	−2.419	0.010
4	11	−1.369727	−15.067	−0.015
5	9	−1.140444	−10.264	0.012
6	6	−1.212500	−7.275	0.001
7	1	−1.248000	−1.248	0.003

TABLE 4 Mean NDVI anomaly by drought severity class.

Drought class	Mean NDVI anomaly	SD	Number of months
Extreme	−0.005	0.020	2
Severe	−0.003	0.006	10
Moderate	−0.005	0.014	45
Mild	0.002	0.024	47

precipitation and ERA5-Land potential evapotranspiration. The results indicate that vegetation dynamics are characterized by a long-term greening trend with substantial interannual variability associated with drought. While vegetation productivity was strongly linked to short-term moisture availability, delayed responses to medium- and long-term drought conditions highlight the importance of drought legacy effects and ecosystem memory in shaping vegetation dynamics.

4.1 Long-term vegetation dynamics and greening trends

The significant positive trend in NDVI observed between 2000 and 2024 indicates an overall increase in vegetation greenness in the Jebel Marra region during this period. Similar greening trends have been reported throughout large portions of the African Sahel and have frequently been attributed to partial rainfall recovery following the severe droughts of the late twentieth century, improved water availability, vegetation regeneration, and changing land-use patterns (Brandt et al., 2015; Dardel et al., 2014; Herrmann et al., 2005).

Several factors may be associated with the observed greening trends. Regional studies have linked vegetation recovery in the Sahel to partial rainfall recovery, changes in land-use practices, and natural vegetation regeneration (Brandt et al., 2015; Dardel et al., 2014). Similar processes may have contributed to the vegetation dynamics in

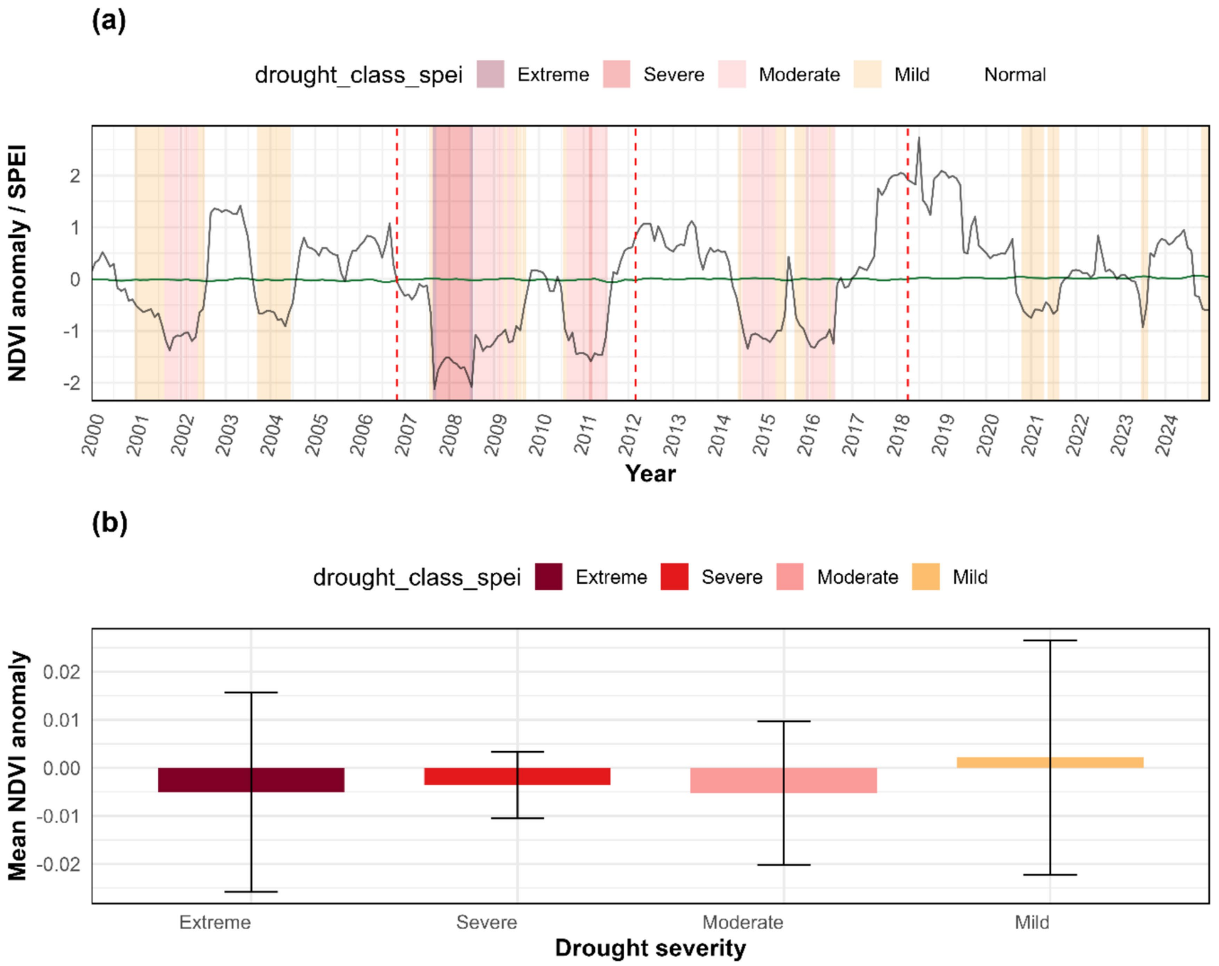

FIGURE 5
Temporal evolution of **(a)** NDVI anomalies, drought severity, and BFAST breakpoints, and **(b)** vegetation response across drought severity classes.

Jebel Marra. However, because this study did not explicitly quantify rainfall trends, land-use change, agricultural abandonment, or conflict-related disturbances, the relative contributions of these factors cannot be determined from the present analysis. However, despite the positive long-term trend, NDVI anomalies revealed recurrent periods of vegetation decline that were associated with drought. This coexistence of long-term greening and episodic vegetation stress suggests that apparent ecosystem recovery does not necessarily imply increased resilience. Similar patterns have been documented in the Sahel, where vegetation greening occurs alongside persistent vulnerability to hydroclimatic extremes (Fensholt et al., 2012; Measho et al., 2021). Importantly, because conflict-related land-use changes were not explicitly quantified in this study, the relative contributions of climatic and anthropogenic drivers could not be disentangled. Consequently, the observed greening trend should be interpreted as the result of potentially interacting environmental and socioecological processes in this region.

4.2 Vegetation responses to multi-scale drought conditions

The analysis revealed that vegetation greenness was most strongly associated with short-term drought conditions, as indicated by the SPEI-3. The contemporaneous correlation between NDVI and SPEI-3 was positive and statistically significant, indicating that vegetation productivity rapidly responds to short-term fluctuations in moisture availability. This finding is consistent with previous studies demonstrating that vegetation dynamics in semi-arid ecosystems are strongly controlled by seasonal precipitation and soil moisture conditions during the growing season (Hua et al., 2019; Vicente-Serrano et al., 2013; Zhang et al., 2023).

In contrast, the contemporaneous relationships between NDVI and both SPEI-6 and SPEI-12 were weak and statistically insignificant. Furthermore, the effective degree-of-freedom correction confirmed that the SPEI-12 relationship remained non-significant after accounting for temporal autocorrelation effects. These findings indicate that contemporaneous vegetation greenness was more closely associated with short-term moisture variability than with concurrent medium- or long-term drought conditions during the study period.

However, lagged analyses have revealed a more complex ecological response. Correlations with SPEI-3 increased substantially and reached a maximum approximately 2 months after drought conditions, whereas those with SPEI-6 exhibited the strongest relationship after approximately 3 months. In contrast, SPEI-12 remained weak throughout the lag period and became statistically significant only after 4–6 month lag. Because both NDVI and SPEI exhibit strong seasonal cycles, part of the observed lag structure may reflect seasonal covariation in addition to the ecological processes. These results demonstrate that the strength and timing of vegetation–drought relationships varied across drought accumulation periods, with stronger delayed associations observed for SPEI-3 and SPEI-6 than for SPEI-12.

Although delayed associations were observed in the lagged analyses, additional anomaly-based analyses suggested that part of the lag structure may reflect the strong seasonal cycle shared by vegetation activity and hydroclimatic conditions. Therefore, the observed lagged relationships should be interpreted cautiously as temporal associations rather than direct evidence of ecological drought-memory mechanisms. Following rainfall deficits, vegetation may continue to function temporarily by utilizing stored soil moisture before the drought impacts are fully expressed in canopy greenness. Similar drought-memory effects have been documented in dryland ecosystems worldwide and are increasingly recognized as important controls of ecosystem resilience and recovery (Jiang et al., 2023; Liu, 2024; Okoduwa and Mokhtarisabet, 2025). The rolling correlation analyses further demonstrated that the vegetation–drought relationships were not temporally stable. However, vegetation sensitivity varied over time, with a stronger coupling occurring during major drought episodes. This finding suggests that ecosystem responses to climate variability intensify under prolonged hydroclimatic stress and may reflect fluctuations in ecosystem resilience.

The drought severity analysis did not identify statistically significant differences in NDVI anomalies among the SPEI-based drought classes. Although the mean NDVI anomalies varied slightly among the severity categories, these differences were small relative to within-class variability and were based on limited sample sizes for the most severe drought categories. Consequently, vegetation responses could not be reliably distinguished among drought severity classes using the available data. This result suggests that drought duration, timing, and antecedent environmental conditions may be at least as important as drought severity in influencing vegetation dynamics in this study area.

4.3 Vegetation regime shifts and ecosystem sensitivity

The BFAST analysis identified three major vegetation breakpoints in 2006–2007, 2012, and 2018. Sensitivity analyses using multiple BFAST parameterizations ($h = 0.10$, 0.15, and 0.20) consistently detected these breakpoints, demonstrating that the identified regime shifts were robust and not artifacts of model configuration.

The identified breakpoints occurred during periods that also contained negative SPEI values and vegetation anomalies in the study area. However, temporal correspondence alone does not establish a causal relationship between drought conditions and vegetation regime shifts. Structural breakpoints detected by BFAST indicate statistically significant changes in the temporal behavior of the vegetation time series and may reflect changes in ecosystem functioning, disturbance regimes, climatic variability, or land-use dynamics (Ddorico et al., 2019; Verbesselt et al., 2010).

Dryland ecosystems are particularly susceptible to threshold-type responses because repeated drought exposure can gradually erode ecological resilience, reduce regeneration capacity, and alter vegetation composition (Bernardino, 2021; Bilal and Gupta, 2025). The persistence of the identified breakpoints across multiple BFAST configurations suggests that the vegetation dynamics in Jebel Marra experienced substantial structural changes during the study period.

However, caution is warranted when attributing these shifts to droughts. The study region has experienced prolonged armed conflict, displacement, land abandonment, and changes in land-use practices during the same period. Although drought likely contributed to vegetation change, the observed breakpoints may also reflect combined climatic and anthropogenic influences that could not be separated within the scope of this study.

4.4 Seasonal vegetation responses and phenological disruption

Seasonal analyses demonstrated that vegetation productivity was consistently lower during drought periods, with the largest reductions occurring during the peak growing season from July to September. This pattern indicates that lower vegetation greenness during drought periods was most evident during the peak growing season, coinciding with the period of maximum seasonal vegetation activity in the region.

In semi-arid ecosystems, the growing season is highly dependent on the timing, duration, and distribution of rainfall events (Nicholson et al., 2013). Moisture deficits during critical growth periods can suppress leaf development, reduce photosynthetic activity, and shorten the duration of active vegetation growth. Consequently, drought may have disproportionate effects on annual biomass production even when total seasonal rainfall reductions are relatively modest (Eziz et al., 2017; Shi et al., 2014). The wider distribution of NDVI values observed during the drought periods was consistent with the spatial variability in vegetation responses across the landscape in the study area. Such variability is expected in mountainous environments where elevation gradients generate substantial differences in microclimate, soil moisture availability, and vegetation composition. The complex topography of Jebel Marra likely creates localized ecological refugia that partially buffer drought impacts in some locations while intensifying stress in others.

These findings highlight the importance of considering topographic heterogeneity when assessing the impacts of drought on montane dryland ecosystems. Future studies integrating spatially explicit vegetation analyses, higher-resolution drought datasets, and field observations will provide valuable insights into the mechanisms governing ecosystem resilience across the Jebel Marra landscape in Sudan.

4.5 Study limitations

Several limitations should be considered when interpreting the findings of this study.

First, although Landsat imagery provides a valuable long-term record of vegetation dynamics at a moderate spatial resolution (30 m), its 16-day revisit interval and cloud contamination, particularly during the rainy season, can introduce temporal gaps in NDVI time series. In this study, missing observations accounted for approximately 5.4% of the monthly records and were addressed using interpolation and smoothing. While sensitivity analyses indicated that the principal temporal patterns were robust, some short-term vegetation fluctuations may not have been fully considered in the study area. In addition, breakpoint detection was conducted using a Savitzky–Golay–smoothed NDVI series, and the sensitivity of breakpoint identification to alternative smoothing approaches (e.g., STL or Whittaker filtering) has not been evaluated.

Second, the NDVI time series was derived from multiple Landsat sensors (TM, ETM+, and OLI). Although Landsat Collection 2 Surface Reflectance products provide substantial radiometric consistency among sensors, explicit cross-sensor harmonization coefficients (e.g., Roy et al., 2016) were not applied in this study. To evaluate the potential influence of the Landsat 7–8 transition, a transition analysis was performed and identified modest differences between sensor-specific NDVI observations; however, the regression-based transition test detected no significant step change after accounting for the long-term temporal trend ($\beta = 0.0076$, $p = 0.462$). Furthermore, the principal BFAST breakpoints occurred in 2006–2007, 2012, and 2018 rather than directly at the Landsat 8 transition in 2013. These results suggest that the major temporal patterns identified in the NDVI record are unlikely to be artifacts of sensor replacement. Nevertheless, residual uncertainty associated with the absence of explicit cross-sensor harmonization cannot be completely excluded and should be considered when interpreting the magnitude of long-term vegetation trends and multi-sensor comparisons.

Third, NDVI primarily represents vegetation greenness and photosynthetic activity and does not directly quantify aboveground biomass, net primary productivity, vegetation structure, or species composition. Consequently, the observed changes in NDVI may not fully reflect the underlying ecological processes such as woody encroachment, species turnover, shifts in vegetation functional types, or changes in ecosystem conditions. Emerging vegetation metrics, such as the near-infrared reflectance of vegetation (NIRv) and kernel NDVI (kNDVI), may provide complementary information and should be explored in future studies.

Fourth, the complex topography of Jebel Marra may generate substantial spatial heterogeneity in hydroclimatic conditions that are difficult to fully represent using gridded climate data. Although the SPEI was derived from high-resolution CHIRPS precipitation and ERA5-Land potential evapotranspiration data, uncertainties associated with PET estimation remain. Previous studies have reported that ERA5-Land may overestimate atmospheric evaporative demand in some arid and semi-arid environments, which may influence drought magnitude estimates in these regions. Consequently, some local vegetation responses to drought may not be fully reflected in the regional-scale analyses presented in this study.

Future research would benefit from adopting a multi-indicator drought assessment framework that integrates meteorological and ecological drought metrics with complementary environmental and socio-economic indicators. In addition to the SPEI, indices such as the Standardized Precipitation Index (SPI) and Palmer Drought Severity Index (PDSI) provide additional perspectives on drought dynamics. Furthermore, integrating land-use and land-cover change data, wildfire occurrence records, agricultural productivity indicators, and conflict-related datasets could improve the attribution of vegetation changes to climatic and non-climatic drivers. This approach has been recommended in recent drought-risk assessments and may provide a more comprehensive understanding of ecosystem vulnerability in the Jebel Marra region (İpek and Kahya, 2025).

Fifth, this study focused primarily on the climatic controls of vegetation dynamics and did not explicitly quantify the effects of land-use change, grazing pressure, fire occurrence, agricultural abandonment, or conflict-related disturbances. Given the prolonged socio-political instability in Darfur since the early 2000s, the vegetation trajectories in Jebel Marra likely reflect the interactions between climatic and anthropogenic drivers. Future studies integrating displacement data, conflict-event databases, land-use change analyses, and field observations would provide a more comprehensive understanding of vegetation change in the region.

Sixth, the drought severity analysis should be interpreted with caution. Although differences in the mean NDVI anomalies were observed among the drought categories, statistical testing revealed no significant differences between the drought severity classes. Moreover, the number of observations within the extreme ($n = 2$) and severe ($n = 10$) drought categories was limited, which reduced statistical power. Consequently, the influence of drought severity on vegetation responses remains uncertain and warrants further investigation using longer time series data and additional drought events. Furthermore, both the NDVI and SPEI exhibit strong seasonal cycles. Although temporal autocorrelation was explicitly accounted for in the lagged-correlation analysis, the possibility that some lagged relationships partly reflect seasonal covariation rather than direct drought responses cannot be completely excluded.

Finally, the correlation-based analyses employed in this study did not establish causality. Vegetation dynamics in dryland ecosystems are influenced by multiple interacting climatic, ecological, and socio-economic factors. Therefore, the observed relationships should be interpreted as statistical associations rather than direct causal effects.

Despite these limitations, this study provides a robust regional-scale assessment of drought–vegetation interactions in one of the most environmentally and politically vulnerable regions of the African Sahel. The integration of long-term Landsat observations, locally derived drought indices, lagged response analyses, and breakpoint detection provides valuable insights into ecosystem dynamics and resilience under increasing climatic variability.

5 Conclusion

This study investigated vegetation dynamics and drought relationships in the Jebel Marra highlands of western Sudan using Landsat-derived NDVI time series and locally derived multi-scale SPEI indices based on CHIRPS precipitation and ERA5-Land potential evapotranspiration for the period of 2000–2024. By integrating trend analysis, lagged correlation assessment, seasonal evaluation, and breakpoint detection, this study provides a regional-scale assessment of vegetation variability and drought conditions in a climatically sensitive dryland mountain environment.

The results identified a significant long-term increase in vegetation greenness during the study period despite substantial interannual variability and recurrent drought episodes. Periods of reduced vegetation activity occurred throughout the record and frequently coincided with negative SPEI conditions during the study period.

Among the examined drought timescales, NDVI exhibited the strongest contemporaneous relationship with short-term drought conditions, as represented by SPEI-3. In contrast, contemporaneous relationships with SPEI-6 and SPEI-12 were weak and statistically non-significant. Lagged-correlation analyses identified stronger delayed associations for SPEI-3 and SPEI-6, whereas relationships with SPEI-12 remained weak after accounting for temporal autocorrelation.

Breakpoint detection identified three persistent changes in the NDVI time series occurring around 2006–2007, 2012, and 2018. Sensitivity testing demonstrated that these breakpoints remained stable across multiple BFAST parameterizations, supporting the robustness of the detected structural changes.

Seasonal analyses showed lower NDVI values during drought periods across most months of the year, with the largest differences occurring from July to September. However, drought severity classes were not associated with statistically significant differences in NDVI anomalies, suggesting that vegetation variability was not clearly differentiated among the examined drought severity categories.

Overall, the findings demonstrate that vegetation dynamics in Jebel Marra were more closely associated with short-term moisture variability than with concurrent long-term drought conditions in the region. The integration of Landsat observations, locally derived drought indicators, and breakpoint analysis provides a useful framework for monitoring vegetation changes and hydroclimatic variability in dryland mountain environments.

Future research should integrate higher-temporal-resolution satellite observations, field-based ecological measurements, land-use and conflict datasets, and multiple drought indicators (e.g., SPI, SPEI, and PDSI) to improve our understanding of the interacting influences of climatic variability, environmental change, and human activities on ecosystem dynamics across the Jebel Marra landscape.

Data availability statement

The datasets presented in this study can be found in online repositories. The names of the repository/repositories and accession number(s) can be found at: DOI 10.5281/zenodo.20683145.

Author contributions

AA: Conceptualization, Data curation, Formal analysis, Investigation, Methodology, Project administration, Software, Validation, Visualization, Writing – original draft, Writing – review & editing. KC: Supervision, Writing – review & editing.

Funding

The author(s) declared that financial support was not received for this work and/or its publication

Acknowledgments

We extend our heartfelt thanks to the Sudanese Ministry of Higher Education and Scientific Research and the University of Gezira for their invaluable academic support. We also appreciate the Tempus Public Foundation and the University of Sopron for awarding a PhD scholarship to the first author of this study. Additionally, we are grateful to the Landsat team for supplying the satellite data.

Conflict of interest

The author(s) declared that this work was conducted in the absence of any commercial or financial relationships that could be construed as a potential conflict of interest.

Generative AI statement

The author(s) declared that Generative AI was used in the creation of this manuscript. During the preparation of this manuscript, the authors used generative artificial intelligence (AI) tools to assist with language editing, grammar correction, and improvement of manuscript readability. The AI tools were not used for data analysis, interpretation of results, generation of scientific conclusions, or decision-making. All scientific content, analyses, interpretations, and conclusions presented in this manuscript were developed, verified, and approved by the authors, who take full responsibility for the accuracy and integrity of the work.

Any alternative text (alt text) provided alongside figures in this article has been generated by Frontiers with the support of artificial intelligence and reasonable efforts have been made to ensure accuracy, including review by the authors wherever possible. If you identify any issues, please contact us.

Publisher's note

All claims expressed in this article are solely those of the authors and do not necessarily represent those of their affiliated organizations, or those of the publisher, the editors and the reviewers. Any product that may be evaluated in this article, or claim that may be made by its manufacturer, is not guaranteed or endorsed by the publisher.

Supplementary material

The Supplementary material for this article can be found online at: https://www.frontiersin.org/articles/10.3389/ffgc.2026.1879552/full#supplementary-material

References

Abdul-Jalil, M., and Unruh, J. D. (2013). Land rights under stress in Darfur: a volatile dynamic of the conflict. *War Soc.* 32, 156–181. doi: 10.1179/0729247313Z

Agustiyara, A., Timár, G., and Székely, B. (2026). "Multi-factor fire susceptibility index (FSI) in Hungary: a data-driven approach using remotely sensed data for peri-urban and forested landscapes." *Model. Earth Syst. Environ.* 2026 12:144. doi:10.1007/S40808-026-02785-W.

Ahmed, A. A. (1983). Forest reserves and woodland savanna regeneration on the sub-Saharan massif of Jebel Marra, democratic Republic of the Sudan. *Vegetatio* 54, 65–78. doi: 10.1007/BF00035142

Ahmed, A., Rotich, B., and Czimber, K. (2024). Assessment of the environmental impacts of conflict-driven internally displaced persons: a Sentinel-2 satellite based analysis of land use/cover changes in the Kas locality, Darfur, Sudan. *PLoS One* 19:e0304034. doi: 10.1371/journal.pone.0304034

Ahmed, A., Rotich, B., and Czimber, K. (2025). Climate change as a double-edged sword: exploring the potential of environmental recovery to foster stability in Darfur, Sudan. *Climate* 13:63. doi: 10.3390/CLI13030063

Ahmed, A., Rotich, B., Kipkulei, H. K., and Czimber, K. (2026). Vegetation recovery amid conflicts: analysis of land use land cover changes in Darfur, Sudan, using high-resolution satellite imagery. *Heliyon* 12:e45086. doi: 10.1016/J.HELIYON.2026.E45086

Ahmed, A., Rotich, B., Kipkulei, H. K., Lameck, A. S., Gallai, B., and Czimber, K. (2025). Vegetation dynamics and climate variability in conflict zones: a case study of Sortony internally displaced camp, Darfur, Sudan. *Land* 14:1680. doi: 10.3390/LAND14081680

Ali, H. (2014). *Surface Water-Harvesting for Agricultural Production in Darfur*. eds. I. Elbadawi and A. A. Ali 59–88.

Alriah, M. A. A., Bi, S., Nkunzimana, A., Elameen, A. M., Sarfo, I., and Ayugi, B. (2024). Assessment of observed changes in drought characteristics and recent vegetation dynamics over arid and semiarid areas in Sudan. *Theor. Appl. Climatol.* 155, 3541–3561. doi: 10.1007/S00704-023-04824-3/FIGURES/11

Anyamba, A., and Tucker, C. J. (2005). Analysis of Sahelian vegetation dynamics using NOAA-AVHRR NDVI data from 1981–2003. *J. Arid Environ.* 63, 596–614. doi: 10.1016/J.JARIDENV.2005.03.007

Bernardino, P. (2021) "*Understanding Turning Points in Dryland Ecosystem Functioning - ProQuest*." Available online at: https://www.proquest.com/openview/c328d832041f1a9588c90645c44c860e/1?cbl=2026366&diss=y&pq-origsite=gscholar (Accessed April 20, 2026).

Bilal, S. B., and Gupta, V. (2025). Tracing vegetation resilience and recovery pathways to drought through time series decomposition. *Hydrol. Process.* 39:e70208. doi: 10.1002/HYP.70208

Blauhut, V., Stahl, K., Stagge, J. H., Tallaksen, L. M., De Stefano, L., and Vogt, J. (2016). Estimating drought risk across Europe from reported drought impacts, drought indices, and vulnerability factors. *Hydrol. Earth Syst. Sci.* 20, 2779–2800. doi: 10.5194/HESS-20-2779-2016

Brandt, M., Mbow, C., Diouf, A. A., Verger, A., Samimi, C., and Fensholt, R. (2015). Ground- and satellite-based evidence of the biophysical mechanisms behind the greening Sahel. *Glob. Chang. Biol.* 21, 1610–1620. doi: 10.1111/gcb.12807

Bunting, E. L., Munson, S. M., and Villarreal, M. L. (2017). Climate legacy and lag effects on dryland plant communities in the southwestern U.S. *Ecol. Indic.* 74, 216–229. doi: 10.1016/J.ECOLIND.2016.10.024

Chen, J., Jönsson, P., Tamura, M., Gu, Z., Matsushita, B., and Eklundh, L. (2004). A simple method for reconstructing a high-quality NDVI time-series data set based on the Savitzky–Golay filter. *Remote Sens. Environ.* 91, 332–344. doi: 10.1016/J.RSE.2004.03.014

Dai, A. (2011). Characteristics and trends in various forms of the palmer drought severity index during 1900-2008. *J. Geophys. Res. Atmos.* 116:12115. doi: 10.1029/2010JD015541

Dardel, C., Kergoat, L., Hiernaux, P., Mougin, E., Grippa, M., and Tucker, C. J. (2014). Re-greening Sahel: 30 years of remote sensing data and field observations (Mali, Niger). *Remote Sens. Environ.* 140, 350–364. doi: 10.1016/J.RSE.2013.09.011

Ddorico, P., Rosa, L., Bhattachan, A., and Okin, G. S. (2019). "Desertification and land degradation," in *Dryland Ecohydrology*, eds. P. D'Odorico, A. Porporato and C. W. Runyan 573–602.

Dutra, A. C., Srivastava, A., Ganem, K. A., Arai, E., Huete, A., and Shimabukuro, Y. E. (2025). Remote sensing-based phenology of dryland vegetation: contributions and perspectives in the southern hemisphere. *Remote Sens.* 17:2503. doi: 10.3390/RS17142503

El Kenawy, A. M. (2024). "Hydroclimatic extremes in arid and semi-arid regions: status, challenges, and future outlook," in *Hydroclimatic Extremes in the Middle East and North Africa: Assessment, Attribution and Socioeconomic Impacts*, eds. A. M. El Kenawy, I. A. Ismail, and M. F. Abdelwahab 1–22.

Eziz, A., Yan, Z., Tian, D., Han, W., Tang, Z., and Fang, J. (2017). Drought effect on plant biomass allocation: a meta-analysis. *Ecol. Evol.* 7, 11002–11010. doi: 10.1002/ECE3.3630

FAO (2015) *Sudan of action (2015–2019) summary*. Available online at: https://openknowledge.fao.org/server/api/core/bitstreams/3670890d-87fb-4501-94df-b3cd51fb28c4/content (Accessed April 20, 2026).

Fathi-Taperasht, A., Shafizadeh-Moghadam, H., Sadian, A., Xu, T., and Nikoo, M. R. (2023). Drought-induced vulnerability and resilience of different land use types using time series of MODIS-based indices. *Int. J. Disaster Risk Reduct.* 91:103703. doi: 10.1016/J.IJDRR.2023.103703

Fensholt, R., Langanke, T., Rasmussen, K., Reenberg, A., Prince, S. D., Tucker, C., et al. (2012). Greenness in semi-arid areas across the globe 1981–2007 — an earth observing satellite based analysis of trends and drivers. *Remote Sens. Environ.* 121, 144–158. doi: 10.1016/J.RSE.2012.01.017

Funk, C., Peterson, P., Landsfeld, M., Pedreros, D., Verdin, J., Shukla, S., et al. (2015). The climate hazards infrared precipitation with stations - a new environmental record for monitoring extremes. *Sci. Data* 2:150066. doi: 10.1038/SDATA.2015.66

Gorelick, N., Hancher, M., Dixon, M., Ilyushchenko, S., Thau, D., and Moore, R. (2017). Google earth engine: planetary-scale geospatial analysis for everyone. *Remote Sens. Environ.* 202, 18–27. doi: 10.1016/J.RSE.2017.06.031

Hegazy, A. K., Hosni, H. A., Kabiel, H. F., Badawi, E. S. M., Emam, M. H., and Lovett-Doust, L. (2018a). Population ecology of some keystone tree species in the Jebel Marra region of Darfur. *Rend. Lincei* 29, 659–673. doi: 10.1007/s12210-018-0701-z

Hegazy, A. K., Kabiel, H. F., Hosni, H. A., Badawi, E. S. M., and Lovett-Doust, L. (2018b). Spatial and temporal variation in plant community phenology in the Jebel Marra region of Darfur. *Folia Geobot.* 53, 389–403. doi: 10.1007/s12224-018-9333-4

Herrmann, S. M., Anyamba, A., and Tucker, C. J. (2005). Recent trends in vegetation dynamics in the African Sahel and their relationship to climate. *Glob. Environ. Change* 15, 394–404. doi: 10.1016/J.GLOENVCHA.2005.08.004

Hua, L., Wang, H., Sui, H., Wardlow, B., Hayes, M. J., and Wang, J. (2019). Mapping the spatial-temporal dynamics of vegetation response lag to drought in a semi-arid region. *Remote Sens.* 11:1873. doi: 10.3390/RS11161873

IPCC (2023) *Integration of Climate Change Adaptation in Land Use Planning*. Available online at: https://climate-adapt.eea.europa.eu/en/metadata/adaptation-options/adaptation-of-integrated-land-use-planning (Accessed May 10, 2025).

İpek, A. F., and Kahya, E. (2025). Integrating spatio-probabilistic mapping and remote sensing for comprehensive drought risk assessment. *Model. Earth Syst. Environ.* 12:43. doi: 10.1007/S40808-025-02696-2

Jiang, P., Wang, Y., Yang, Y., Gu, X., Huang, Y., Liu, L., et al. (2023). Spatiotemporal features and time-lagged effects of drought on terrestrial ecosystem in Southwest China. *Forests* 14:781. doi: 10.3390/F14040781

Kamta, F. N., Schilling, J., and Scheffran, J. (2020). Insecurity, resource scarcity, and migration to camps of internally displaced persons in Northeast Nigeria. *Sustainability* 12:6830. doi: 10.3390/SU12176830

Knight, J. (2023). "The hydrology and Palaeohydrology of the Central Sahara," in *World Geomorphological Landscapes Part F2043*, eds. J. Knight and S. Kröpelin 99–109.

Kusch, E., Davy, R., and Seddon, A. W. R. (2022). Vegetation-memory effects and their association with vegetation resilience in global drylands. *J. Ecol.* 110, 1561–1574. doi: 10.1111/1365-2745.13891

Liu, W. (2024). "The response of NDVI to drought at different temporal scales in the Yellow River Basin from 2003 to 2020." *Water* 2024, Vol. 16:2416. doi:10.3390/W16172416

Liu, X., Ji, L., Zhang, C., and Liu, Y. (2022). A method for reconstructing NDVI time-series based on envelope detection and the Savitzky-Golay filter. *Int. J. Digit. Earth* 15, 553–584. doi: 10.1080/17538947.2022.2044397

Ma, J., Zhang, C., Guo, H., Chen, W., Yun, W., Gao, L., et al. (2020). Analyzing ecological vulnerability and vegetation phenology response using NDVI time series data and the BFAST algorithm. *Remote Sens.* 12, 1–21. doi: 10.3390/RS12203371

Measho, S., Chen, B., Pellikka, P., Guo, L., Zhang, H., Cai, D., et al. (2021). Assessment of vegetation dynamics and ecosystem resilience in the context of climate change and drought in the horn of Africa. *Remote Sens.* 13:1668. doi: 10.3390/RS13091668

Mehmood, K., Anees, S. A., Muhammad, S., Hussain, K., Shahzad, F., Liu, Q., et al. (2024). Analyzing vegetation health dynamics across seasons and regions through NDVI and climatic variables. *Sci. Rep.* 14:11775. doi: 10.1038/s41598-024-62464-7

Muñoz-Sabater, J., Dutra, E., Agustí-Panareda, A., Albergel, C., Arduini, G., Balsamo, G., et al. (2021). ERA5-land: a state-of-the-art global reanalysis dataset for land applications. *Earth Syst. Sci. Data* 13, 4349–4383. doi: 10.5194/ESSD-13-4349-2021

Nicholson, E. S., Acs, F., Bordi, I., and Wang, D. (2013). The west African Sahel: a review of recent studies on the rainfall regime and its interannual variability. *Wiley Online Library* 2013, 1–32. doi: 10.1155/2013/453521

Okoduwa, A. K., and Mokhtarisabet, S. (2025). "Spatiotemporal analysis of drought in the Sahelian region of northeastern Nigeria, sub-Saharan Africa." *Theor. Appl. Climatol.* 2025 156:293. doi: 10.1007/s00704-025-05542-8

Pettorelli, N., Vik, J. O., Mysterud, A., Gaillard, J. M., Tucker, C. J., and Stenseth, N. C. (2005). Using the satellite-derived NDVI to assess ecological responses to environmental change. *Trends Ecol. Evol.* 20, 503–510. doi: 10.1016/J.TREE.2005.05.011

R Core Team (2020) *R: The R Project for Statistical Computing*. Available online at: https://www.r-project.org/ (Accessed May 16, 2026).

Rouse, J. W., Haas, R. H., Deering, D. W., Schell, J. A., and Harlan, J. C. (1974). *Monitoring the Vernal Advancement and Retrogradation (Green Wave Effect) of Natural Vegetation*.

Roy, D. P., Kovalskyy, V., Zhang, H. K., Vermote, E. F., Yan, L., Kumar, S. S., et al. (2016). Characterization of Landsat-7 to Landsat-8 reflective wavelength and normalized difference vegetation index continuity. *Remote Sens. Environ.* 185, 57–70. doi: 10.1016/J.RSE.2015.12.024

Shi, Z., Thomey, M. L., Mowll, W., Litvak, M., Brunsell, N. A., Collins, S. L., et al. (2014). Differential effects of extreme drought on production and respiration: synthesis and modeling analysis. *Biogeosciences* 11, 621–633. doi: 10.5194/BG-11-621-2014

Shi, G., Wei, D., Qi, M., Zhang, Z., Niu, H., Zhang, Y., et al. (2026). Frequent dry-hot extremes slow the loss of semi-arid ecosystem resilience. *Glob. Chang. Biol.* 32:e70835. doi: 10.1111/GCB.70835

Stringer, L. C., Mirzabaev, A., Benjaminsen, T. A., Harris, R. M. B., Jafari, M., Lissner, T. K., et al. (2021). Climate change impacts on water security in global drylands. *One Earth* 4, 851–864. doi: 10.1016/J.ONEEAR.2021.05.010

UNEP (2024). *Sudan Post-Conflict Environmental Assessment | UNEP - UN Environment Programme*. Available online at: https://www.unep.org/sudan/sudan-post-conflict-environmental-assessment (Accessed April 1, 2026).

van Deetjen, L. (2020) "*Management of Conflict-Induced Internally Displaced Persons in a "Post-Conflict" Context: A Comparative Case Study of Uganda and South Sudan*." Available online at: https://urn.kb.se/resolve?urn=urn:nbn:se:lnu:diva-100436 (Accessed February 1, 2026).

Verbesselt, J., Hyndman, R., Zeileis, A., and Culvenor, D. (2010). Phenological change detection while accounting for abrupt and gradual trends in satellite image time series. *Remote Sens. Environ.* 114, 2970–2980. doi: 10.1016/J.RSE.2010.08.003

Vicente-Serrano, S., Beguería, S., López-Moreno, J. I., Vicente-Serrano, S. M., Beguería, S., and López-Moreno, J. I. (2010). A multiscalar drought index sensitive to global warming:

the standardized precipitation evapotranspiration index. *J. Clim.* 23, 1696–1718. doi: 10.1175/2009JCLI2909.1

Vicente-Serrano, S. M., Gouveia, C., Camarero, J. J., Beguería, S., Trigo, R., López-Moreno, J. I., et al. (2013). Response of vegetation to drought time-scales across global land biomes. *Proc. Natl. Acad. Sci.* 110, 52–57. doi: 10.1073/pnas.1207068110

Wang, X., Wang, Z., Pan, P., Liu, X., Li, G., Wang, Z., et al. (2026). Evaluating ecosystem water use efficiency under drought stress: a case study of the Helan Mountain region, Northwest China. *Landsc. Ecol.* 41:66. doi: 10.1007/S10980-026-02312-3

Williams, M. (2021). *When the Sahara Was Green: How Our Greatest Desert Came to Be*, 1–272.

Wulder, M. A., Loveland, T. R., Roy, D. P., Crawford, C. J., Masek, J. G., Woodcock, C. E., et al. (2019). Current status of Landsat program, science, and applications. *Remote Sens. Environ.* 225, 127–147. doi: 10.1016/J.RSE.2019.02.015

Yao, Y., Liu, Y., Fu, Y., Zhang, X., Wang, L., and Liu, R. (2025). Detect changes in marsh plant communities based on Landsat long time series data and BFAST model. *Land Degrad. Dev.* 37, 1353–1367. doi: 10.1002/ldr.70177

Ye, Y., Coops, N. C., Wulder, M. A., and Hermosilla, T. (2025). A multi-resolution forest stand segmentation algorithm integrating Landsat imagery and forest structural, age, and species attributes. *ISPRS J. Photogramm. Remote Sens.* 226, 381–395. doi: 10.1016/J.ISPRSJPRS.2025.05.023

Zeng, Y., Hao, D., Huete, A., Dechant, B., Berry, J., Chen, J. M., et al. (2022). Optical vegetation indices for monitoring terrestrial ecosystems globally. *Nat. Rev. Earth Environ.* 2022 3:7 3, 477–493. doi: 10.1038/s43017-022-00298-5

Zhang, J., Ding, J., Hou, X., and Wu, P. (2023). Quantifying drought response sensitivity and spatial and temporal heterogeneity of vegetation in arid and semi-arid regions. *Int. J. Remote Sens.* 44, 1665–1683. doi: 10.1080/01431161.2023.2182651